

# Anisotropic spin-fluctuations in SmCoPO revealed by $^{31}\text{P}$ NMR measurement

Mayukh Majumder<sup>1</sup>, K. Ghoshray<sup>1</sup>, A. Ghoshray<sup>1</sup>, Anand Pal<sup>2</sup>, and V.P.S. Awana<sup>2</sup>

<sup>1</sup>*ECMP Division, Saha Institute of Nuclear Physics*

<sup>2</sup>*Quantum Phenomenon and Applications Division,  
National Physical Laboratory (CSIR)*

$^{31}\text{P}$  NMR spectral features in polycrystalline SmCoPO reveal an axially symmetric local magnetic field. At low temperature, the anisotropy of the internal magnetic field increases rapidly, with  $K_{ab}$  increasing faster than that of  $K_c$ . The dominant contribution to this anisotropy arises from Sm-4*f* electron contribution over that of Co-3*d*. The intrinsic width  $2\beta$  deviates from linearity with respect to bulk susceptibility below 170 K due to the enhancement of  $(1/T_2)_{\text{dynamic}}$ , which along with the continuous increase of anisotropy in the internal magnetic field is responsible for the wipe out effect of the NMR signal, well above  $T_C$ .  $1/T_1$  shows large anisotropy confirming a significant contribution of Sm-4*f* electron spin fluctuations to  $1/T_1$ , arising from indirect RKKY type exchange interaction indicating a non-negligible hybridization between Sm-4*f* orbitals and the conduction band, over the itinerant character of the Co-3*d* spins. This anisotropy originates from the orientation dependence of  $\chi''(\mathbf{q}, \omega)$ . The 3*d*-spin fluctuations in the *ab* plane is 2D FM in nature, while along the *c*-axis, a signature of a weak 2D AFM spin fluctuations superimposed on weak FM spin-fluctuations even in a field of 7 T and far above  $T_N$  is observed. The enhancement of this AFM fluctuations of the Co-3*d* spins along *c*-axis, at further low temperature is responsible to drive the system to an AFM ordered state.

PACS numbers:

## I. INTRODUCTION

The unconventional nature of the iron based (grouped in several families) superconductors has drawn immense attention from the theoreticians as well as experimentalists.<sup>1</sup> Presence of strongly correlated electrons are responsible for diverse electronic and magnetic properties shown by these materials. The non-superconducting parent compounds also show interesting properties<sup>2,3</sup> such as spin density wave (SDW) transition, structural phase transition, itinerant ferromagnetism etc. Several members of these families show superconductivity (SC) upon carrier doping. In 1111 and 122 family, superconductivity can be achieved by Co doping in place of iron.<sup>4,5</sup> It is presumed that the study of Co based non superconducting members may provide useful information about the key factor that determines the ground state i.e. either SC or magnetic.

The magnetic property of the *RECoAsO* (*RE* = rare earth) series has been investigated<sup>4,6-14</sup> for both non-magnetic (La), and magnetic (Ce, Pr, Sm, Nd, and Gd) members, the *RECoPO* on the other hand has been reported for LaCoPO<sup>6,15-17</sup> and CeCoPO.<sup>18</sup> Both these compounds exhibit only ferromagnetic transition due to Co-3*d* electrons with  $T_C = 35$  K and 75 K respectively. The Ce-ions are on the border to magnetism with a Kondo scale of  $T_K \sim 40$  K with enhanced Sommerfield coefficient of  $\gamma = 200 \text{ mJ/molK}^2$ . In *RECoAsO* series, La, Ce, and Pr show paramagnetic (PM) to ferromagnetic (FM) transition,<sup>8</sup> whereas Sm, Nd, and Gd show PM  $\rightarrow$  FM  $\rightarrow$  antiferromagnetic (AFM) transition.<sup>8,13</sup> The AFM transition was proposed to be mediated by the interaction between the *RE*-4*f* and the Co-3*d* electrons.

Furthermore, in SmCoAsO and NdCoAsO a second AFM transition only due to *RE* ion was also reported.<sup>10,14</sup> Recently it has been shown from magnetization and specific heat measurements that Sm/NdCoPO also undergo three magnetic transitions i.e.  $T_{C,Co}$  (80 K), the Sm<sup>4*f*}-Co<sup>3*d*}/Nd<sup>4*f*}-Co<sup>3*d*}</sup> interplayed AFM transition ( $T_{N1}$ ) below 20 K and finally Sm<sup>3+</sup>/Nd<sup>3+</sup> spins individual AFM transitions at ( $T_{N2}$ )=5.4/2.0 K.<sup>19</sup> The important difference between these two series is that in *RECoAsO*, the  $T_C$  increases from La to Ce and remains unchanged for Pr - Gd, whereas in *LCoPO* family, the  $T_C$  increases progressively as we go down the series from La to Sm. Thus the strength of the exchange interactions changes as one replaces As by P. In both the series, the lattice volume decreases across the series. In general, with the application of chemical or physical pressure,  $T_C$  decreases due to the increment of density of state (DOS) at Fermi level (magneto-volume effect). However, due to the lattice size decrement, the three dimensionality of the magnetic interaction may enhance causing an increment of  $T_C$ , thereby confirming the active role of the competing phenomena governing the actual ground state.</sup></sup></sup>

Our earlier  $^{31}\text{P}$  and  $^{139}\text{La}$  NMR measurements in grain aligned (*c*||*H*<sub>0</sub>) LaCoPO (quasi 2D Fermi surface) reveal that the spin fluctuation of 3*d* electrons in PM state is basically two dimensional (2D) in nature with non negligible 3D part and it is 3D in the FM state.<sup>15,17</sup> Moreover, relaxation rate shows weak anisotropy. Since SmCoPO has the minimum unit cell volume in this series, it would be interesting to study the paramagnetic state to probe the interplay between increasing interlayer interaction due to three dimensionality of the Fermi surface (causes increment of  $T_C$ ) and magneto-volume effect (causes decrement of  $T_C$ ). Probing dynamic spin susceptibility, the

spin-lattice relaxation rate provides microscopic information on the dimensionality of spin-fluctuations. We would thus examine a few pertinent questions: (i) is the decrement of lattice volume in SmCoPO low enough to make the spin-fluctuation 3D in nature even in the paramagnetic state? (ii) Whether any anisotropy is expected in the nuclear relaxation rate in SmCoPO because the contributions of different 3d orbitals of Co and 4f orbitals of Sm to the Fermi surface, governing nuclear relaxation, would change as a result of the lattice shrinkage? and (iii) to understand the mechanism which drives the FM oriented Co-3d spins to reorder antiferromagnetically at further low temperature which persists even in a field of 14 T.

## II. EXPERIMENTAL

Polycrystalline samples of SmCoPO and LaCoPO were synthesized by solid state reaction the details of which are described in<sup>19</sup>. The powder sample was characterized using x-ray diffraction technique with CuK $\alpha$  radiation at room temperature in a Rigaku X-ray diffractometer. The Rietveld analysis of the X-ray powder diffraction data confirmed that the samples are crystallized in tetragonal phase with all the peaks indexed to the space group P4/nmm. The  $^{31}\text{P}$  NMR measurements were carried out in powder samples of SmCoPO and LaCoPO, using a conventional phase-coherent spectrometer (Thamway PROT 4103MR) with a 7.0 T ( $H_0$ ) superconducting magnet (Bruker). The temperature variation study was performed in an Oxford continuous flow cryostat equipped with a ITC503 controller. The spectrum was recorded by changing the frequency step by step and recording the spin echo intensity by applying a  $\pi/2 - \tau - \pi/2$  solid echo pulse sequence. Shifts were measured with respect to the  $^{31}\text{P}$  resonance line position ( $\nu_R$ ) in  $\text{H}_3\text{PO}_4$  solution. The spin-lattice relaxation time ( $T_1$ ) was measured using the saturation recovery method, applying a single  $\pi/2$  pulse. The spin-spin relaxation time ( $T_2$ ) was measured applying  $\pi/2 - \tau - \pi$  pulse sequence.

## III. RESULTS AND DISCUSSIONS

### A. $^{31}\text{P}$ NMR spectra in SmCoPO

The Hamiltonian for the interaction between the nuclear and electronic spins in the presence of external field  $H_0$  can be written as

$$H = -\gamma\hbar\mathbf{I}\cdot\mathbf{H}_0 + \sum_j \mathbf{I}\cdot\mathbf{A}_j\cdot\mathbf{S}_j + \sum_j \gamma\hbar\mathbf{I}\cdot\boldsymbol{\mu}_B g\mathbf{S}_j \frac{3\cos^2\theta_j - 1}{r_j^3}, \quad (1)$$

where the first term is the nuclear Zeeman energy, the second term represents hyperfine interaction with jth magnetic ion having spin  $\mathbf{S}_j$  and the third term denotes the dipolar interaction. In the most general case, when

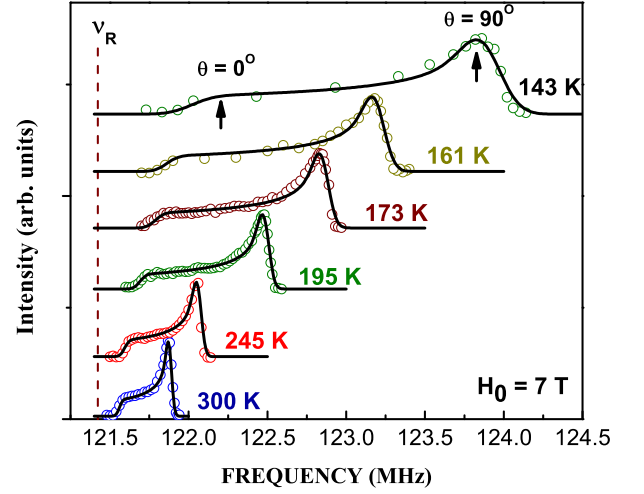


FIG. 1: Typical  $^{31}\text{P}$  NMR spectrum ( $\circ$ ) in SmCoPO. Vertical dashed line represents reference position. Continuous lines correspond to the simulated spectrum derived from eq. 3 using Gaussian line shape. The vertical arrows indicate step ( $\theta = 0^\circ$ ) and maximum ( $\theta = 90^\circ$ ) respectively.

a nucleus experiences a completely anisotropic internal magnetic field (sum of the hyperfine and dipolar field), the resonance frequency in a single crystal is given by<sup>20</sup>

$$\nu = \nu_R [1 + K_{iso} + K_{ax}(3\cos^2\theta - 1) + K_{aniso}\sin^2\theta\cos^2 2\phi], \quad (2)$$

where  $K_{iso} = (K_1 + K_2 + K_3)/3$ ,  $K_{ax} = (2K_3 - K_1 - K_2)/6$ , and  $K_{aniso} = (K_2 - K_1)/2$ .  $K_1$ ,  $K_2$ , and  $K_3$  are the principal components of the total shift tensor. If a nucleus experiences an internal field of cylindrical symmetry, the third term in eq. (2) vanishes, since  $K_1 \approx K_2$ .

In a polycrystalline specimen, the crystallites being oriented randomly, the anisotropic shift results in a broadening proportional to the applied field. Since all values of  $u = \cos\theta$  are equally probable the expression for the line shape would be  $p(\nu) \sim 1/|d\nu/du|$ . Superimposing a gaussian broadening of width  $2\beta$ , to the resonance line from each of the crystallites, the line shape in polycrystalline sample will be

$$I(\nu') = \int_{-\infty}^{\infty} p(\nu) \exp[-(\nu - \nu')^2/2\beta^2] d\nu. \quad (3)$$

The shift parameters  $K_{iso}$ ,  $K_{ax}$  and linewidth ( $2\beta$ ) can be obtained by fitting the spectra using eq. (3).

Figure 1 shows some typical  $^{31}\text{P}$  NMR spectra in polycrystalline SmCoPO at different temperatures. The resonance line shape corresponds to a powder pattern for a spin  $I = 1/2$  nucleus experiencing an axially symmetric local magnetic field, as expected for SmCoPO having tetragonal symmetry. The step in the low-frequency side corresponds to  $H_0 \parallel c$  ( $\theta = 0^\circ$ ) and the maximum in high frequency side corresponds to  $H_0 \perp c$  ( $\theta = 90^\circ$ ). The shift of the step with respect to the reference po-

sition ( $\nu_R$ ), corresponds to  $K_c$  and that of the maximum corresponds to  $K_{ab}$ , where  $K_{iso} = \frac{2}{3}K_{ab} + \frac{1}{3}K_c$  and  $K_{ax} = \frac{1}{3}(K_c - K_{ab})$ . The continuous line superimposed on each experimental line is the calculated spectrum corresponding to eq. 3 using Gaussian line shape. Most important feature is that the separation between the step,  $K_c$  and the maximum,  $K_{ab}$  increases at low temperature along with line broadening. In particular,  $K_{ab}$  shows much larger change than that of  $K_c$ . Finally, the resonance line could not be detected below 130 K, ( $T_C$  at  $H=7$  T is about 110 K as determined from the derivative of the  $\chi$  versus  $T$  curve; not shown here). The line did not reappear till the lowest temperature. Such thing did not happen in case of  $^{31}\text{P}$  and  $^{139}\text{La}$  NMR studies in  $\text{LaCoPO}$ , where the resonance line was detected<sup>17</sup> even below  $T_C$ .

### 1. $^{31}\text{P}$ NMR wipe out and spin-spin relaxation rate $1/T_2$

Figure 2 shows the variation of  $2\beta$  with the bulk magnetic susceptibility,  $\chi$  (with temperature as implicit parameter) in  $\text{SmCoPO}$ , depicting a linear  $\chi$  dependence of  $2\beta$  in the range 173-300 K. This arises mainly from the contribution due to the demagnetizing field. Below this range there is a significant deviation from linearity, showing a large enhancement. To get a more quantitative picture,  $^{31}\text{P}$  spin-spin relaxation time ( $T_2$ ) also known as the transverse relaxation time was measured, as a function of temperature (inset (b) of Fig. 2). In this measurement, the echo integral (which arises from the transverse magnetization) was taken as a function of time delays ( $\tau$ ) between two  $rf$  pulses. The recovery of the transverse magnetization was found to be exponential at all temperatures.  $T_2$  was obtained by fitting the equation  $M(2\tau) = M_0 \exp(-2\tau/T_2)$ , (solid lines in the inset (a) in Figure 2.) where  $M_0$  is the initial magnetization. At any temperature, the magnitude of  $T_2$  remains same when measured at the position of the maximum ( $\theta = 90^\circ$ ) and at the step ( $\theta = 0^\circ$ ) respectively, indicating its isotropic nature.

In general,  $1/T_2$  can be written as the sum of the contribution from (i) dipolar interaction between the nuclear magnetic moments which is temperature and field independent ( $1/T_2|_{static}$ ) and (ii) the dipolar and hyperfine interactions of the nuclei with the longitudinal component of the fluctuating magnetic field produced by the neighboring  $\text{Co}^{2+}$   $3d$ -spins and  $\text{Sm}$   $4f$ -spins. This dynamic part  $1/T_2|_{dynamic}$ , is temperature dependent, when the fluctuation frequency becomes close to nuclear resonance frequency below a certain temperature, due to the development of short range correlation among the electronic spins as  $T_C$  is approached. In weak collision fast motion approximation, one can express  $1/T_2|_{dynamic}$ , in terms of the spectral density of the spin-fluctuating hyperfine field at zero frequency,<sup>21,22</sup>

$$1/T_2|_{dynamic} = \gamma_n^2 \langle \delta H_z^2 \rangle \tau(T) + 1/2T_1 \quad (4)$$

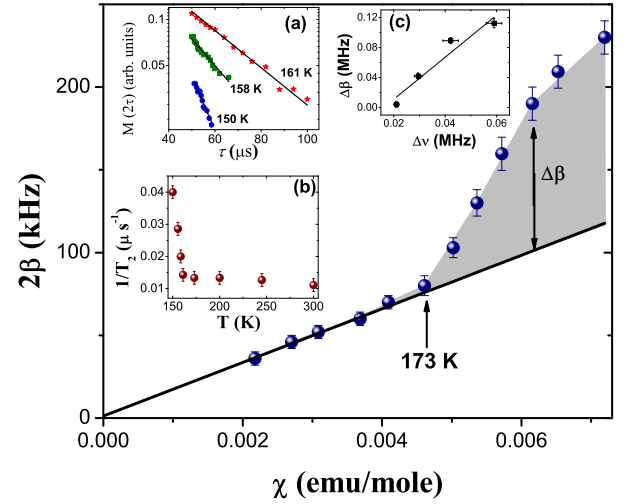


FIG. 2: The variation of  $2\beta$  against magnetic susceptibility (solid circle) in  $\text{SmCoPO}$ , solid line is the linear fit. Inset (a): recovery of transverse magnetization at different temperatures, solid lines corresponds to  $M(2\tau) = M_0 \exp(-2\tau/T_2)$ ; (b)  $1/T_2 (\mu\text{s}^{-1})$  versus temperature; (c):  $\Delta\nu$  (MHz) versus  $\Delta\beta$  (MHz), solid line is the linear fit as discussed in the text.

where  $\delta H_z$  is the local longitudinal field originating from a magnetic moment sitting at a distance  $r$  apart from the probed nuclear spin, and  $\tau$  stands for correlation time, which is only determined by the dynamics of the exchanged coupled magnetic ions. Therefore, the observed  $\theta$  independent behavior of  $T_2$ , as mentioned above indicates that the longitudinal component of the fluctuating electronic magnetic field at the  $^{31}\text{P}$  nuclear site is isotropic in nature. It is to be noted that the intrinsic width,  $2\beta$  in Eq. 3 contains sum of the contributions from  $1/T_2|_{static}$ ,  $1/T_2|_{dynamic}$  and that due to the demagnetizing field. Among them the first contribution is magnetic field independent while the second and third depend on field and the magnetic susceptibility.<sup>23</sup>

The contribution  $2\beta_{dynamic}$  to the total  $2\beta$  was estimated, by subtracting the contribution due to the linear part determined from the extrapolated values (larger  $\chi_M$  values in Fig. 2) from  $2\beta$ . In the inset (c) of Fig. 2, we have plotted this  $2\beta_{dynamic}$  denoted as  $\Delta\beta$  versus the line width ( $\Delta\nu$ ) obtained from the measured  $T_2$ . The linear behavior confirms that the observed large enhancement of  $2\beta$  below 173 K arises due to the enhancement of  $1/T_2$  or more specifically  $(1/T_2)_{dynamic}$ . As  $T_2$  reaches a value of  $25 \mu\text{s}$  at 150 K, there is a possibility that at lower temperature, it becomes so short that one has to apply a delay time  $\tau$  between the two  $rf$  pulses ( $\pi/2 - \tau - \pi/2$ ) used to observe the spin echo, which is comparable to or shorter than the dead time of the spectrometer. As a consequence, the NMR signal coming from the  $^{31}\text{P}$  nuclei can not be digitized by the spectrometer, resulting the whole signal to vanish.

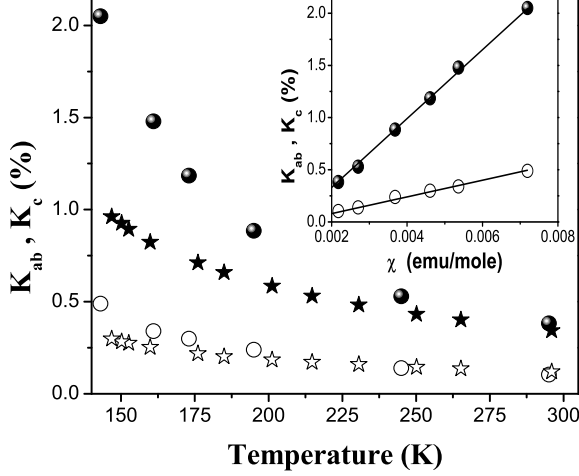


FIG. 3:  $K_{ab}$ ,  $K_c$  vs temperature for SmCoPO (filled circle and open circle respectively) and  $K_{ab}$ ,  $K_c$  vs temperature for LaCoPO (filled star and open star respectively), Inset shows  $K_{ab}$ ,  $K_c$  vs  $\chi$  for SmCoPO and the solid line is the linear fit.

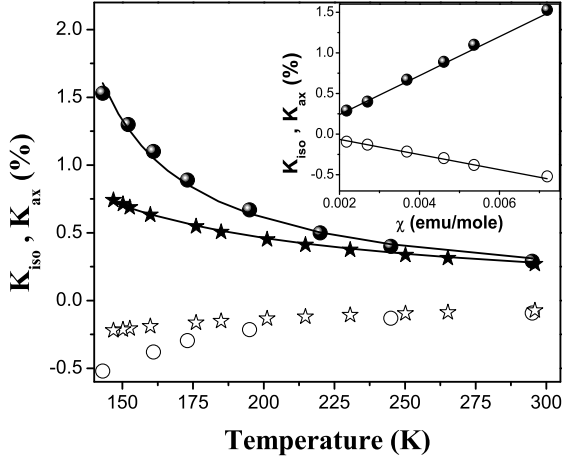


FIG. 4:  $K_{iso}$ ,  $K_{ax}$  vs temperature for SmCoPO (filled circle and open circle respectively) and  $K_{iso}$ ,  $K_{ax}$  vs temperature for LaCoPO (filled star and open star respectively), solid lines correspond to Eq. 6. Inset shows  $K_{iso}$ ,  $K_{ax}$  vs  $\chi$  for SmCoPO and the solid line is the linear fit.

### B. Knight shift and hyperfine field

Figures 3 and 4 show temperature dependence of shift parameters  $K_c$ ,  $K_{ab}$ ,  $K_{iso}$  and  $K_{ax}$  in SmCoPO and the same in LaCoPO for comparison. Around 300 K, shift parameters for LaCoPO and SmCoPO are of same magnitude, however, at low temperature,  $K_{ab}$ ,  $K_c$ ,  $K_{iso}$  and  $K_{ax}$  for SmCoPO increases rapidly than in LaCoPO. Measured shift can be written as  $K = K_0 + K(T)$ , where  $K_0$  is the temperature independent contribution arising from conduction electron spin susceptibility, orbital susceptibility and diamagnetic susceptibility of core

electrons.  $K(T)$  arises from the temperature dependent susceptibility due to Co-3d and Sm-4f spins,

$$K(T) = (H_{hf}/N\mu_B)\chi(T) \quad (5)$$

$H_{hf}$  is the total coupling constant due to the electron nuclear hyperfine and dipolar interactions,  $N$  is the avogadro number and  $\mu_B$  is the Bohr magneton. Insets of Figs. 3 and 4 show linear variation of  $K_c$ ,  $K_{ab}$ ,  $K_{iso}$  and  $K_{ax}$  with  $\chi = M/H$ . From these plots the obtained values of the coupling constants are  $H_{hf}^{ab}$ ,  $H_{hf}^c$ ,  $H_{hf}^{iso}$ ,  $H_{hf}^{ax}$  are 18.4, -4.46, 13.4 and -5.19 kOe/ $\mu_B$  respectively. Using the atomic coordinates of Sm, Co and P,  $H_{dip}^{ax}$  (-0.44 kOe/ $\mu_B$ ) at the  $^{31}\text{P}$  site was calculated from Eq. 9 of sec.III.C. The value is one order of magnitude smaller than that of experimental  $H_{hf}^{ax}$ . Thus the observed temperature dependent anisotropic part of the shift is mainly due to the hyperfine interaction. If we consider that the contribution to  $K_{ax}$  due to Co-3d electrons is nearly same in LaCoPO and SmCoPO, then the observed larger enhancement of  $K_{ax}$  in SmCoPO at low temperature compared to that in LaCoPO ( Fig. 4) is a signature of more pronounced contribution of Sm-4f electrons over that of Co-3d for producing anisotropic local magnetic field at the  $^{31}\text{P}$  site.

Temperature dependence of  $K_{iso}$  can be well described by the Curie-Weiss type behavior,

$$K_{iso}(T) = (H_{hf}^{iso}/N\mu_B) \frac{C}{(T - \theta)} \quad (6)$$

as represented by the continuous line in figure 4 for LaCoPO and SmCoPO. The estimated  $P_{eff}$  value from Curie-Weiss constant ( $C$ ) are  $1.4\mu_B$  with  $\theta=53$  K for LaCoPO and  $1.65\mu_B$  with  $\theta=110$  K for SmCoPO, which are in close agreement with those determined from magnetic susceptibility data.<sup>19</sup> This indicates that there is a contribution of Sm 4f moment over that of Co 3d moment even in the paramagnetic state. It is to be noted that in NdFeAsO<sub>1-x</sub>F<sub>x</sub> and CeCoAsO the  $^{75}\text{As}$  Knight shift<sup>24,25</sup> was found to be influenced by 4f moments though As is situated in a different plane. A notable difference between FeAs based systems and CoP/CoAs based systems is that the hyperfine field at the  $^{75}\text{As}$  site in LaFeAsO<sub>(1-x)</sub>F<sub>x</sub> is temperature independent and the temperature dependence appears only when La is replaced by other rare earths.<sup>24,26</sup> Whereas, in CoP/CoAs based systems, the hyperfine field is temperature dependent even in LaCoPO<sup>15,16</sup> and LaCoAsO<sup>12</sup>. Substitution of other rare earth gives an additional temperature dependent contribution to the shift arising from 4f electrons superimposed on that due to Co 3d electrons.

### C. Nuclear spin-lattice relaxation rate $1/T_1$

$1/T_1$  was determined from the recovery of the longitudinal component of the nuclear magnetization  $M(\tau)$  as a

function of the delay time  $\tau$  using equation

$$M(\tau) = M(\infty)(1 - \exp^{-\tau/T_1}) \quad (7)$$

for nuclear spin  $I=1/2$ . The recovery curves (inset (a) of Fig. 5) were found to be exponential throughout the whole temperature range, as expected for an ensemble of  $I=1/2$  nuclei with a common spin temperature. This confirms good sample homogeneity with negligible amount of phosphorous containing impurity phase. The temperature dependence of the  $^{31}\text{P}$  nuclear spin-lattice relaxation rates  $(1/T_1)_{ab}$  and  $(1/T_1)_c$  in SmCoPO (inset(b) of Fig. 5) in the temperature range 140 - 300 K clearly show the anisotropic nature. The  $T_1$  values in SmCoPO are one order of magnitude shorter than that in LaCoPO near 300 K and becomes two orders of magnitude shorter near 140 K. In case of SmFeAsO $_{1-x}$ F $_x$   $^{19}\text{F}$  NMR<sup>26</sup> relaxation rate  $(1/T_1)$  was three orders of magnitude higher than that in LaFeAsO $_{1-x}$ F $_x$ .<sup>27</sup> This enhancement in  $1/T_1$  was also observed in case of  $^{75}\text{As}$   $1/T_1$  in 1111 superconductor with Pr and Nd as rare earth element.<sup>28</sup> The enhancement in  $1/T_1$  was assigned due to the  $4f$  electrons and not due to the Fe  $3d$  electrons. Prando et al.<sup>26</sup> have concluded that the increment of  $1/T_1$  from 200 K in SmFeAsO $_{1-x}$ F $_x$  was due to the Sm  $4f$  electrons via the indirect RKKY exchange coupling and which indicates that there is a non-negligible hybridization between Sm  $4f$  with conduction electrons i.e. the  $4f$  electrons are not fully localized in nature. In SmCoPO the large enhancement in magnitude of  $1/T_1$  at low temperature with respect to that in LaCoPO should also arise due to the contribution of Sm  $4f$  electrons through the magnetic dipolar interaction and the hyperfine interaction (through RKKY type conduction electron mediated  $c-f$  exchange) over the contribution of Co  $3d$  electrons (which is also present in LaCoPO). Moreover, the continuous enhancement of  $1/T_1$  in SmCoPO from below 300 K, indicates the signature of the development of short range correlation far above  $T_C$ . This should be characteristic of itinerant magnetism of both Co  $3d$  and Sm  $4f$  electrons.<sup>29</sup> So  $^{31}\text{P}$  will feel the effect of itinerant Co  $3d$  via the hybridization between Co  $3d$  and P  $2p$  and also feel the effect of Sm  $4f$  electrons via RKKY interaction through the conduction electrons along with the magnetic dipolar interaction with the same.

Contribution to spin-lattice relaxation rate due to  $4f$  spin fluctuation (from Sm) via the dipolar coupling<sup>30</sup> is

$$(1/T_1)_{\text{dip}} = \frac{\sqrt{2}\pi\gamma_n^2(g\mu_B)^2}{6\omega_e} J(J+1) \sum_i r_i^{-6} \times [F_i(\alpha_i, \beta_i, \gamma_i) + F'_i(\alpha_i, \beta_i, \gamma_i)], \quad (8)$$

where  $F_i(\alpha_i, \beta_i, \gamma_i)$  and  $F'_i(\alpha_i, \beta_i, \gamma_i)$  are geometrical factors which depend on  $\alpha_i, \beta_i, \gamma_i$ , the direction cosines of  $r_i$  connecting the  $i$ -th Sm atom and  $^{31}\text{P}$  nuclear spin with respect to the principal axes of the dipolar field tensor. Using the structural parameters<sup>19</sup> for SmCoPO we have calculated the dipolar field at the  $^{31}\text{P}$  nuclear site arising

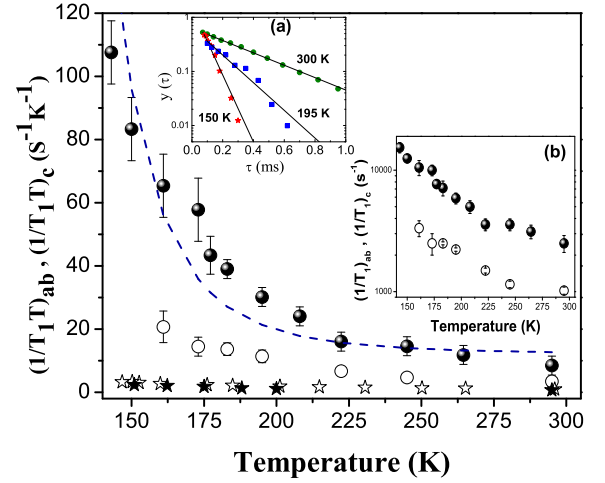


FIG. 5:  $(1/T_1T)_{ab}$  (filled circle),  $(1/T_1T)_c$  (open circle) versus  $T$  for SmCoPO and  $(1/T_1T)_{ab}$  (filled star),  $(1/T_1T)_c$  (open star) versus  $T$  for LaCoPO. The dashed line corresponds to Eq. 16. Inset(a): recovery curves at different temperatures where  $y(\tau) = \frac{M(\infty) - M(\tau)}{M(\infty)}$  and Inset (b):  $(1/T_1)_{ab}$  (filled circle) and  $(1/T_1)_c$  (open circle) vs  $T$  for SmCoPO.

from Sm moment with the formula,

$$H_{\text{dip}} = \mu \sum \frac{(3r_j r_k - r^2 \delta_{jk})}{r^5}; j, k = x, y, z \quad (9)$$

$\mu$  is the magnetic moment of Sm moment. The direction of the principal components of the dipolar tensor coincide with the crystallographic axes system and this makes calculation of  $F_i(\alpha_i, \beta_i, \gamma_i)$  and  $F'_i(\alpha_i, \beta_i, \gamma_i)$  simple. Thus the lattice sum of eq. 8

$$\sum_i r_i^{-6} [F_i(\alpha_i, \beta_i, \gamma_i) + F'_i(\alpha_i, \beta_i, \gamma_i)] = 2.143 \times 10^{46} \text{ cm}^{-6}.$$

The electronic exchange frequency  $\omega_e$  is estimated from the Neel temperature ( $T_N = 5.4$  K) of the Sm- $4f$  moment<sup>19</sup> by

$$(\hbar\omega_e)^2 = \frac{1}{6z} \frac{(3k_B T_N)^2}{J(J+1)}. \quad (10)$$

Taking  $z=4$ , number of the nearest neighbor Sm spins  $\omega_e = 1.46 \times 10^{11} \text{ sec}^{-1}$ . Finally,  $(1/T_1)_{\text{dip}} = 434 \text{ sec}^{-1}$ . At 300 K the average value of  $1/T_1$  in SmCoPO for  $\theta=0$  and  $\theta=\pi/2$  is  $\sim 1760 \text{ sec}^{-1}$ . The value of  $1/T_1$  at 300 K in LaCoPO is  $\sim 300 \text{ sec}^{-1}$ . If we now assume that the contribution due to Co- $3d$  spins is nearly same in LaCoPO and SmCoPO, then also  $[(1/T_1)_{\text{SmCoPO}} - (1/T_1)_{\text{LaCoPO}}]$  is more than three times larger than  $(1/T_1)_{\text{dip}}$  for Sm  $4f$  spins i.e. the main contribution to  $1/T_1$  in SmCoPO comes from hyperfine interaction with the Sm- $4f$  spins.

Main panel of Fig. 5 shows the  $(1/T_1T)_{ab}$  and  $(1/T_1T)_c$  vs  $T$  curves in SmCoPO and in LaCoPO. In SmCoPO  $(1/T_1T)_{ab}$  increases much faster than that of

$(1/T_1T)_c$ . Whereas, in LaCoPO this anisotropy is negligible. This enhanced anisotropy is a signature of contribution of anisotropic Sm  $4f$  orbitals along with the Co  $3d$  orbitals. In general,  $(1/T_1T)_{SF}$  is given by

$$(1/T_1T)_{SF} \propto \sum_q |H_{hf}(q)|^2 \chi''(q, \omega_n) / \omega_n \quad (11)$$

where  $\chi''(q, \omega_n)$  is the imaginary part of the transverse dynamical electron spin susceptibility,  $\gamma_n$  and  $\omega_n$  are the nuclear gyromagnetic ratio and Larmor frequency respectively.  $H_{hf}(q)$  is the hyperfine form factor. Terasaki<sup>31</sup> et al. in LaFeAsO<sub>0.7</sub> and Kitagawa<sup>32</sup> et. al. in BaFe<sub>2</sub>As<sub>2</sub> had shown that at P site  $H_{hf}(q)$  is non-zero for  $q = 0$  and also non-zero for  $q \neq 0$  (inplane off-diagonal pseudo-dipolar hyperfine field has a non zero value along  $c$  axis for  $q = (\pm\pi, \pm\pi)$ ).  $q \neq 0$  contribution have been found at As site for BaFe<sub>2</sub>As<sub>2</sub>,<sup>32</sup> SrFe<sub>2</sub>As<sub>2</sub>,<sup>33</sup> LaFeAsO, LaFeAsO<sub>1-x</sub>F<sub>x</sub><sup>34</sup> and also in Co doped BaFe<sub>2</sub>As<sub>2</sub><sup>34-36</sup> systems. This indicates that  $1/T_1T$  at P site can feel ferromagnetic spin-fluctuations as well as antiferromagnetic spin-fluctuations.

The directional dependence in  $(1/T_1T)_{ab}$  and  $(1/T_1T)_c$  can be due to anisotropy in  $H_{hf}$  or due to anisotropy of  $\chi''(q, \omega_n)$ , or both. Inset of Fig. 6 shows that the ratio  $(1/T_1T)_{ab}/(1/T_1T)_c$  is higher than that of the ratio  $[(H_{hf}^{ab})^2 + (H_{hf}^c)^2]/2(H_{hf}^{ab})^2$ , which suggests that there is also a significant anisotropy in  $\chi''(q, \omega_n)$ .  $(1/T_1T)_c$  and  $(1/T_1T)_{ab}$  are related to  $\chi''_{in}$  (in plane) and  $\chi''_{out}$  (out of plane) by the following relations,<sup>37</sup>

$$(1/T_1T)_c \propto \sum_q 2|H_q^{in}|^2 \frac{\chi''_{in}(q, \omega)}{\omega_n}, \quad (12)$$

$$(1/T_1T)_{ab} \propto \sum_q [|H_q^{out}|^2 \frac{\chi''_{out}(q, \omega)}{\omega_n} + |H_q^{in}|^2 \frac{\chi''_{in}(q, \omega)}{\omega_n}], \quad (13)$$

Using these relations, we have estimated  $\chi''_{in}/\omega_n$  and  $\chi''_{out}/\omega_n$ , whose  $T$  dependence are shown in Fig. 6.  $\chi''_{out}/\omega_n$  is about two orders of magnitude higher than  $\chi''_{in}/\omega_n$ . Such anisotropy in relaxation rate was also observed in other FeAs based systems like BaFe<sub>2</sub>As<sub>2</sub>,<sup>32</sup> SrFe<sub>2</sub>As<sub>2</sub>,<sup>33</sup> LaFeAsO, LaFeAsO<sub>1-x</sub>F<sub>x</sub><sup>34</sup> and also Co doped BaFe<sub>2</sub>As<sub>2</sub><sup>34-36</sup> systems. Define  $\mathbf{A} = [(1/T_1T)_{ab}/(1/T_1T)_c]/[(H_{hf}^{ab})^2 + (H_{hf}^c)^2]/2(H_{hf}^{ab})^2$ .  $\mathbf{A}$  will be one if there is no anisotropy in  $\chi''/\omega_n$  and  $\mathbf{A}$  will deviate from unity if anisotropy comes from  $\chi''/\omega_n$ . The values of  $\mathbf{A}$  obtained using the reported <sup>75</sup>As NMR  $T_1$  data in BaFe<sub>2</sub>As<sub>2</sub>, SrFe<sub>2</sub>As<sub>2</sub>, and LaFeAsO are 2.4, 1.75, 1.5 respectively. Also in Co doped BaFe<sub>2</sub>As<sub>2</sub>,  $(1/T_1T)_{ab}/(1/T_1T)_c$  is between 1-2. The value of  $\mathbf{A}$  in case of SmCoPO is 5.66. This clearly indicates a dominant contribution of Sm  $4f$  spin fluctuations over that due to Co- $3d$  electrons, in the anisotropy of  $1/T_1$  in SmCoPO. Anisotropy in spin-fluctuations arises from the spin-orbit coupling for which the spin and orbital degrees of freedom get mixed and dynamic magnetic susceptibility becomes anisotropic. So the preferred directions of

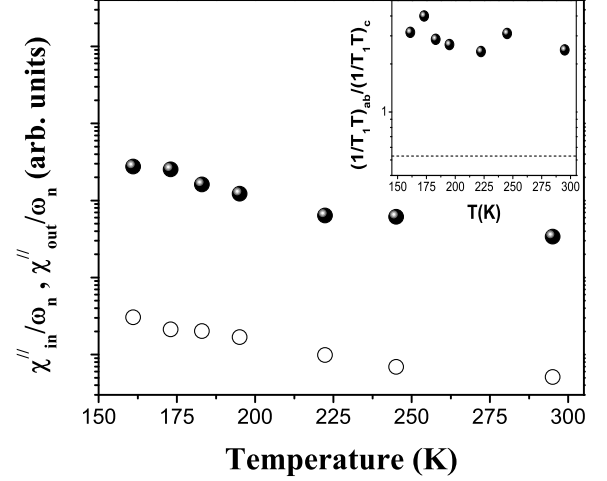


FIG. 6: Variation of  $\chi''_{in}/\omega_n$  (open circle) and  $\chi''_{out}/\omega_n$  (filled circle) with respect to  $T$  for SmCoPO. Inset:  $(1/T_1T)_{ab}/(1/T_1T)_c$  versus  $T$  and the dashed line indicates the value of  $[(H_{hf}^{ab})^2 + (H_{hf}^c)^2]/2(H_{hf}^{ab})^2 \approx 0.53$ .

orbital fluctuations are determined by the geometry and orbital characters of the Fermi surfaces. Band structure calculations using tight-binding approximation is highly needed to evaluate which  $3d$  and  $4f$  orbital fluctuations are responsible for anisotropy in spin-fluctuations in SmCoPO.

When the Knight shift and nuclear spin-lattice relaxation process are governed by conduction electrons,  $1/T_1TK^2$  is constant. If there is an exchange interaction between the electrons then using Stoner approximation along with random phase approximation, modified Korringa relation can be written as<sup>38-40</sup>  $S_0/T_1TK_{spin}^2 = K(\alpha)$ , where  $S_0 = (\hbar/4\pi k_B)(\gamma_e/\gamma_n)^2$  and

$$K(\alpha) = \langle (1 - \alpha_0)^2 / (1 - \alpha_q)^2 \rangle_{FS}. \quad (14)$$

$\alpha_q = \alpha_0 \chi_0(q)/\chi(0)$  is the  $q$ -dependent susceptibility enhancement, with  $\alpha_0 = 1 - \chi_0(0)/\chi(0)$  representing the  $q = 0$  value. The symbol  $\langle \rangle_{FS}$  means the average over  $q$  space on the Fermi surface.  $\chi(0)$  and  $\chi_0(q)$  represents the static susceptibility and the  $q$  mode of the generalized susceptibility of noninteracting electrons respectively.  $K(\alpha) < 1$  means the spin-fluctuations are enhanced around  $q = 0$ , leading to the predominance of ferromagnetic correlations and  $K(\alpha) > 1$  signifies that spin-fluctuations are enhanced away from  $q = 0$ . This would indicate a tendency towards AF ordering (at  $q \neq 0$ ). Inset of Fig. 7. shows that for LaCoPO,  $K(\alpha)_{ab}$  and  $K(\alpha)_c$  are  $< 1$  when calculated at 160 K, which shows the predominance of ferromagnetic spin-fluctuations in both these directions. Whereas, in SmCoPO,  $K(\alpha)_{ab} < 1$  but  $K(\alpha)_c > 1$  (1.8), calculated at 160 K. The values of  $K(\alpha)_{ab}$ ,  $K(\alpha)_c$  for LaCoPO and the value  $K(\alpha)_{ab}$  for SmCoPO suggest that the spin fluctuations are ferromagnetic in nature both in the  $ab$ -plane and along the  $c$  direction in LaCoPO. However, the same in SmCoPO is FM in the



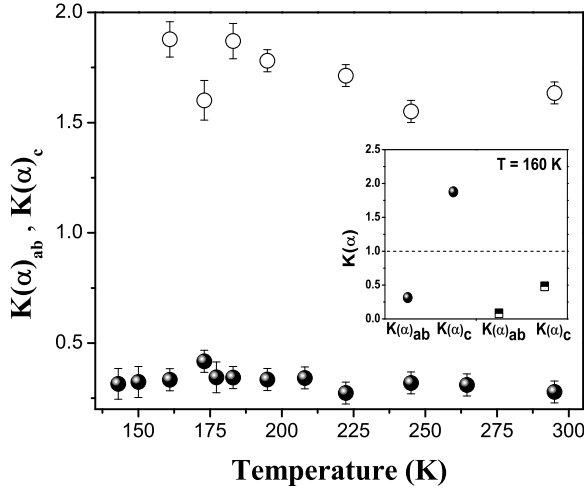


FIG. 7:  $K(\alpha)_{ab}$  (filled circle) and  $K(\alpha)_c$  (open circle) versus  $T$  for SmCoPO. Inset shows  $K(\alpha)_{ab}$ ,  $K(\alpha)_c$  (filled circle) for SmCoPO and  $K(\alpha)_{ab}$ ,  $K(\alpha)_c$  (half-filled square) for LaCoPO at 160 K and the dashed line corresponds to  $K(\alpha) = 1$ .

$ab$ -plane, while along  $c$ -direction there is a signature of the presence of  $q \neq 0$  modes in addition to  $q = 0$  modes. Thus in SmCoPO there exist weak AFM spin-fluctuations along  $c$  axis in contrast to LaCoPO (inset of Fig. 7).

According to the theory of weak itinerant ferromagnet, if 3D/2D spin-fluctuations are dominant<sup>41,42</sup> then  $1/T_1T \propto \chi^{1(3/2)}$ . Fig. 8 shows the  $T$  versus  $(1/T_1TK)_{ab}$  and  $(1/T_1TK^{3/2})_{ab}$  plots revealing dominant 2D FM spin-fluctuations in the  $ab$  plane of SmCoPO particularly in the paramagnetic region.

### 1. Spin fluctuations parameters

Following the theory of Ishigaki and Moriya<sup>42</sup> one can write the imaginary part of dynamic spin susceptibility in terms of the two spin-fluctuation parameters  $T_0$  and  $T_A$  which characterize the width of the spin excitations spectrum in frequency and wave vector ( $\mathbf{q}$ ) space respectively. For ferromagnetic correlations, we have

$$\chi(\mathbf{q}, \omega) = \frac{\pi T_0}{\alpha_Q T_A} \left( \frac{x}{k_B 2\pi T_0 x(y + x^2) - i\omega\hbar} \right), \quad (15)$$

where  $x = \mathbf{q}/q_B$  with  $q_B$  being the effective zone boundary vector,  $\alpha_Q$  a dimensionless interaction constant close to unity for a strongly correlated system,  $y = 1/2\alpha_Q k_B T_A \chi(0, 0)$ . Here the susceptibility is per spin and in units of  $4\mu_B^2$  and has the dimension of inverse of energy,  $T_0$  and  $T_A$  are in Kelvin. From Eq. 11 one can derive  $\chi''(\mathbf{q}, \omega_n)$  in the limit  $\omega_n \rightarrow 0$ , since  $\hbar\omega_n \ll k_B T$ . For 3D spin fluctuations governing the relaxation process, one has to integrate  $\chi''(\mathbf{q}, \omega_n)/\omega_n$ , over a sphere of radius  $\mathbf{q}_B (6\pi^2/v_0)^{1/3}$ , whereas, in case of 2D spin fluctuations, the integration has to be done over a disc of radius  $\mathbf{q}_B (4\pi/v_0)^{1/2}$ .  $v_0$  corresponds to the atomic volume

of Co. So in the latter case

$$1/T_1T = \gamma_n^2 H_{hf}^2 / 4T_A T_0 y^{3/2} + \alpha \quad (16)$$

where according to 2D SCR theory,  $y$  can be approximately written as  $y = (T/6T_0)^{2/3} \exp(-p^2 T_A / 10T)$ , where  $p$  is the ferromagnetic moment in  $\mu_B$  units and  $\alpha$  is the temperature independent contribution of  $1/T_1T$  arising from the orbital moment of  $p$  and  $d$  electrons and the spin of the conduction electrons. Using Eq. 16, we have estimated the spin-fluctuation parameters  $T_A$  and  $T_0$  in SmCoPO as 21000 and 2043 K respectively. The dashed line of Fig. 5 corresponds to Eq. 16.

### 2. Spin fluctuations and possible antiferromagnetic spin-structure

According to the SCR theory of itinerant antiferromagnetism if 3D(2D) spin-fluctuations governs the relaxation process<sup>42</sup> then  $1/T_1T$  is proportional to  $\chi^{1/2(1)}$ . Inset of Fig. 8 shows that  $(1/T_1T)_c$  is nearly proportional to the intrinsic spin susceptibility, probed by NMR shift  $K_c$  (which is proportional to  $\chi_c$ ), which reveals that AFM spin-fluctuations are also nearly 2D in nature. A small slope in this plot could be a signature of the presence of weak FM spin fluctuations superimposed on the weak 2D AFM one along the  $c$ -direction. Presence of FM spin fluctuation along  $c$ -direction due to the inter layer exchange interaction, in the paramagnetic phase in SmCoPO is relevant (observed from  $^{139}\text{La}$  NMR in LaCoPO as shown in<sup>17</sup>) as the FM transition precedes the AFM transition. Possibly this is the reason for which  $\chi''_{in}/\omega_n < \chi''_{out}/\omega_n$ , because  $\chi''_{out}/\omega_n$  arises from the sum of the contributions from  $q = 0$  and  $q \neq 0$  mode of spin-fluctuations. The appearance of weak AFM spin-fluctuations of the Co-3d spins, along  $c$ -direction, far above the ferromagnetic transition (which was absent in case of LaCoPO) is a signature of AF exchange interaction between the Sm-4f and the Co-3d electrons. This is consistent with the fact that Sm-O plane is situated in between two Co-P planes and both are parallel to  $ab$  plane. Due to the presence of AF interaction along  $c$ -direction, though the Co spins in each Co-P plane order ferromagnetically below  $T_C$ , at lower temperature when the AF exchange interaction between the Sm-4f and Co-3d spins, along the  $c$ -direction becomes more stronger, the Co-3d spins in the two adjacent planes would try to align antiparallel even if they remain parallel to each other within a plane. As a result, the system orders antiferromagnetically. Such type of spin structure in NdCoAsO has recently been proposed from elastic neutron scattering study.<sup>10</sup> Signature of the presence of weak AF exchange interaction between the Sm-4f and Co-3d spins even above  $T_C$  obtained from  $^{31}\text{P}$  spin-lattice relaxation data, could possibly be the reason for the persistence of AF transition in SmCoPO even in a magnetic field of 14 T, whereas, it disappears completely at  $H=5$  T in NdCoPO, though the Nd 4f effective moment is higher than that of Sm 4f. As the

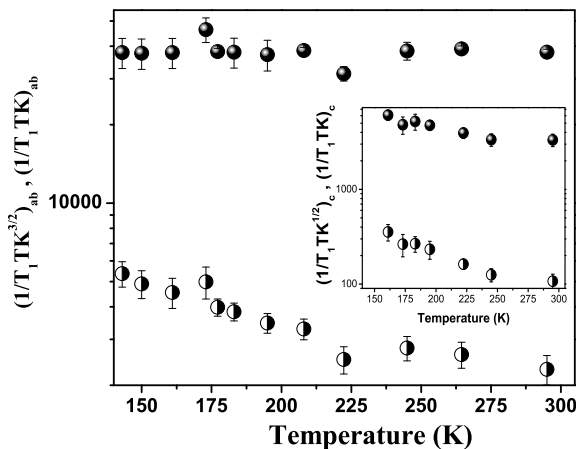


FIG. 8:  $(1/T_1 TK^{3/2})_{ab}$  (filled circle),  $(1/T_1 TK)_{ab}$  (half-filled circle) versus  $T$  for SmCoPO and inset shows  $(1/T_1 TK^{1/2})_c$  (half-filled circle),  $(1/T_1 TK)_c$  (filled circle) versus  $T$  for SmCoPO

lattice parameter  $c$  in SmCoPO is less than that in NdCoPO, therefore, the strength of the AF exchange interaction between Sm-4*f* and Co-3*d* spins present along the  $c$ -direction could be more stronger in SmCoPO than in NdCoPO. Therefore, the  $^{31}\text{P}$  NMR shift and the spin-lattice relaxation studies in other members of LCoPO series would be interesting to understand the effect of the change in the lattice volume, on the nature of the spin fluctuations and as well as the extent of anisotropy, which drives the system to a particular ground state.

#### IV. CONCLUSIONS

We have reported  $^{31}\text{P}$  NMR results in the powder sample of SmCoPO. The spectral features reveal an axially

symmetric nature of the local magnetic field. At low temperature, the anisotropy of the internal magnetic field increases, with  $K_{ab}$  increasing faster than that of  $K_c$ . The intrinsic width  $2\beta$  shows a linear variation with  $\chi_M$  in the range 300 - 170 K. Deviation from linearity below 170 K arises due to the enhancement of  $(1/T_2)_{dynamic}$ . This enhancement of  $(1/T_2)_{dynamic}$  along with the continuous increase of anisotropy in the internal magnetic field is responsible for the wipe out of the NMR signal, well above  $T_C$ . Absence of anisotropy in  $1/T_2$  indicates the isotropic nature of the longitudinal component of the fluctuating local magnetic field.

Observed large anisotropy in  $1/T_1$  of SmCoPO compared to that of LaCoPO, confirms a significant contribution of Sm-4*f* electron arising from indirect RKKY interaction. This indicates a non-negligible hybridization between Sm-4*f* orbitals and the conduction band, over and above the itinerant character of the Co-3*d* spins. The anisotropy of  $1/T_1$  originates mainly from the orientation dependence of  $\chi''(\mathbf{q}, \omega)$ . The 3*d*-spin fluctuations in the  $ab$  plane is primarily of 2D FM in nature similar to that in LaCoPO, while along the  $c$ -axis, a signature of weak 2D AFM spin-fluctuations superimposed on weak FM spin-fluctuations even in a field of 7 T and far above  $T_C$  is observed. The enhancement of this AFM exchange interaction below  $T_C$  should be responsible to drive the Co moment to an AFM ordered state.

- <sup>1</sup> D. C. Johnston, *Advances in Physics* **59**, 803 (2010), and references therein.
- <sup>2</sup> Michael A. McGuire, Andrew D. Christianson, Athena S. Sefat, Brian C. Sales, Mark D. Lumsden, Rongying Jin, E. Andrew Payzant, David Mandrus, Yanbing Luan, Veerle Keppens, Vijayalakshmi Varadarajan, Joseph W. Brill, Raphael P. Hermann, Moulay T. Sougrati, Fernande Grandjean, and Gary J. Long, *Phys. Rev. B* **78**, 094517 (2008).
- <sup>3</sup> Ying Chen, J. W. Lynn, J. Li, G. Li, G. F. Chen, J. L. Luo, N. L. Wang, Pengcheng Dai, C. dela Cruz, and H. A. Mook, *Phys. Rev. B* **78**, 064515 (2008).
- <sup>4</sup> Athena S. Sefat, Ashfia Huq, Michael A. McGuire, Rongying Jin, Brian C. Sales, David Mandrus, Lachlan M. D. Cranswick, Peter W. Stephens, and Kevin H. Stone, *Phys. Rev. B* **78**, 104505 (2008).
- <sup>5</sup> Athena S. Sefat, Rongying Jin, Michael A. McGuire, Brian C. Sales, David J. Singh, and David Mandrus, *Phys. Rev. Lett.* **101**, 117004 (2008).

- <sup>6</sup> Hiroshi Yanagi, Ryuto Kawamura, Toshio Kamiya, Yoichi Kamihara, Masahiro Hirano, Tetsuya Nakamura, Hitoshi Osawa, and Hideo Hosono, *Phys. Rev. B* **77**, 224431 (2008).
- <sup>7</sup> H. Ohta and K. Yoshimura, *Phys. Rev. B* **79**, 184407 (2009).
- <sup>8</sup> H. Ohta and K. Yoshimura, *Phys. Rev. B* **80**, 184409 (2009).
- <sup>9</sup> Andrea Marcinkova, David A. M. Grist, Irene Margiolaki, Thomas C. Hansen, Serena Margadonna, and Jan-Willem G. Bos, *Phys. Rev. B* **81**, 064511 (2010).
- <sup>10</sup> Michael A. McGuire, Delphine J. Gout, V. Ovidiu Garlea, Athena S. Sefat, Brian C. Sales, and David Mandrus, Jr., *Phys. Rev. B* **81**, 104405 (2010).
- <sup>11</sup> H. Ohta, C. Michioka, and K. Yoshimura, *J. Phys. Soc. Jpn.* **79**, 054703, (2010).
- <sup>12</sup> Hiroto Ohta, Chishiro Michioka, Akira Matsuo, Koichi Kindo, and Kazuyoshi Yoshimura, *Phys. Rev. B* **82**, 054421 (2010).



- <sup>13</sup> V. P. S. Awana, I. Nowik, Anand Pal, K. Yamaura, E. Takayama-Muromachi, and I. Felner, Phys. Rev. B **81**, 212501 (2010).
- <sup>14</sup> A. Pal, M. Tropeano, S. D. Kaushik, M. Hussain, H. Kishan, V. P. S. Awana, J. Appl. Phys **109**, 07E121 (2011).
- <sup>15</sup> M. Majumder, K. Ghoshray, A. Ghoshray, B. Bandyopadhyay, B. Pahari, and S. Banerjee, Phys. Rev. B **80**, 212402 (2009).
- <sup>16</sup> H. Sugawara, K. Ishida, Y. Nakai, H. Yanagi, T. Kamiya, Y. Kamihara, M. Hirano, H. Hosono, J. Phys. Soc. Jpn. **78**, 113705 (2009).
- <sup>17</sup> M. Majumder, K. Ghoshray, A. Ghoshray, B. Bandyopadhyay, M. Ghosh, Phys. Rev. B **82**, 054422 (2010).
- <sup>18</sup> C. Krellner, U. Burkhardt, C. Geibel, Physica B **404**, 3206-3209 (2009).
- <sup>19</sup> Anand Pal, S. S. Mehdi, Mushahid Hussain, Bhasker Gahloti and V. P. S. Awana, arXiv:1105.0971 (2011).
- <sup>20</sup> N. Bloembergen, T. J. Rowland, Acta Mater. **1**, 731 (1953).
- <sup>21</sup> C. P. Slichter, *Principles of Magnetic Resonance*, Springer Series in Solid State Sciences 1, (Springer-Verlag, 1992).
- <sup>22</sup> M. Belesi, X. Zong, F. Borsa, C. J. Milios, and S. P. Perlepes, Phys. Rev. B **75**, 064414 (2007).
- <sup>23</sup> W. M. Lomer, Proc. Phys. Soc. **80**, 1380 (1962).
- <sup>24</sup> P. Jeglič, J. -W. G. Bos, A. Zorko, M. Brunelli, K. Koch, H. Rosner, S. Margadonna, and D. Arčon, Phys. Rev. B **79**, 094515 (2009).
- <sup>25</sup> R. Sarkar, A. Jesche, C. Krellner, M. Baenitz, C. Geibel, C. Mazumdar, and A. Poddar, Phys. Rev. B **82**, 054423 (2010).
- <sup>26</sup> G. Prando, P. Carretta, A. Rigamonti, S. Sanna, A. Palenzona, M. Putti, and M. Tropeano, Phys. Rev. B **81**, 100508 (2010).
- <sup>27</sup> K. Ahilan, F. L. Ning, T. Imai, A. S. Sefat, R. Jin, M. A. McGuire, B. C. Sales, and D. Mandrus, Phys. Rev. B **78**, 100501 (2008).
- <sup>28</sup> H. Yamashita, M. Yashima, H. Mukuda, Y. Kitaoka, P. M. Shirage, A. Iyo, Physica C **470**, S375S376 (2010).
- <sup>29</sup> T. Moriya, *Spin Fluctuations in itinerant Electron Magnetism* (Springer-Verlag, New York, 1985).
- <sup>30</sup> T. Moriya, J. Phys. Soc. Jpn. **16**, 23 (1956).
- <sup>31</sup> N. Terasaki, H. Mukuda, M. Yashima, Y. Kitaoka, K. Miyazawa, P. M. Shirage, H. Kito, H. Eisaki, and A. Iyo, J. Phys. Soc. Jpn. **78**, 013701, (2009).
- <sup>32</sup> K. Kitagawa, N. Katayama, K. Ohgushi, M. Yoshida, and M. Takigawa, J. Phys. Soc. Jpn. **77**, 114709 (2008).
- <sup>33</sup> K. Kitagawa, N. Katayama, K. Ohgushi, and M. Takigawa, J. Phys. Soc. Jpn. **78**, 063706 (2009).
- <sup>34</sup> S. Kitagawa, Y. Nakai, T. Iye, K. Ishida, Y. Kamihara, M. Hirano, and H. Hosono, Phys. Rev. B **81**, 212502 (2010).
- <sup>35</sup> F. Ning, K. Ahilan, T. Imai, A. S. Sefat, R. Jin, M. A. McGuire, B. C. Sales, and D. Mandrus, J. Phys. Soc. Jpn. **78**, 013711 (2009).
- <sup>36</sup> F. L. Ning, K. Ahilan, T. Imai, A. S. Sefat, M. A. McGuire, B. C. Sales, D. Mandrus, P. Cheng, B. Shen, and H.-H. Wen, Phys. Rev. Lett. **104**, 037001 (2010).
- <sup>37</sup> K. Ishida, H. Mukuda, Y. Minami, Y. Kitaoka, Z. Q. Mao, H. Fukazawa, Y. Maeno, Phys. Rev. B **64**, 100501(R) (2001).
- <sup>38</sup> T. Moriya, J. Phys. Soc. Jpn. **18**, 516, (1963).
- <sup>39</sup> Albert Narath and H. T. Weaver, Phys. Rev. **175**, 373 (1968).
- <sup>40</sup> Chin-Shan Lue and Joseph H. Ross, Jr., Phys. Rev. B **60**, 8533 (1999).
- <sup>41</sup> M. Hatatani, T. Moriya, J. Phys. Soc. Jpn. **64**, 3434, (1995).
- <sup>42</sup> A. Ishigaki, T. Moriya, J. Phys. Soc. Jpn. **67**, 3924, (1998).